PUBLISHED VERSION

Eleanore Blereau, Tim E. Johnson, Chris Clark, Richard J.M. Taylor, Peter D. Kinny, Martin Hand
Reappraising the P-T evolution of the Rogaland-Vest Agder Sector, southwestern Norway
Geoscience Frontiers, 2017; 8(1):1-14

Originally published at:
http://doi.org/10.1016/j.gsf.2016.07.003

PERMISSIONS

http://creativecommons.org/licenses/by-nc-nd/4.0/

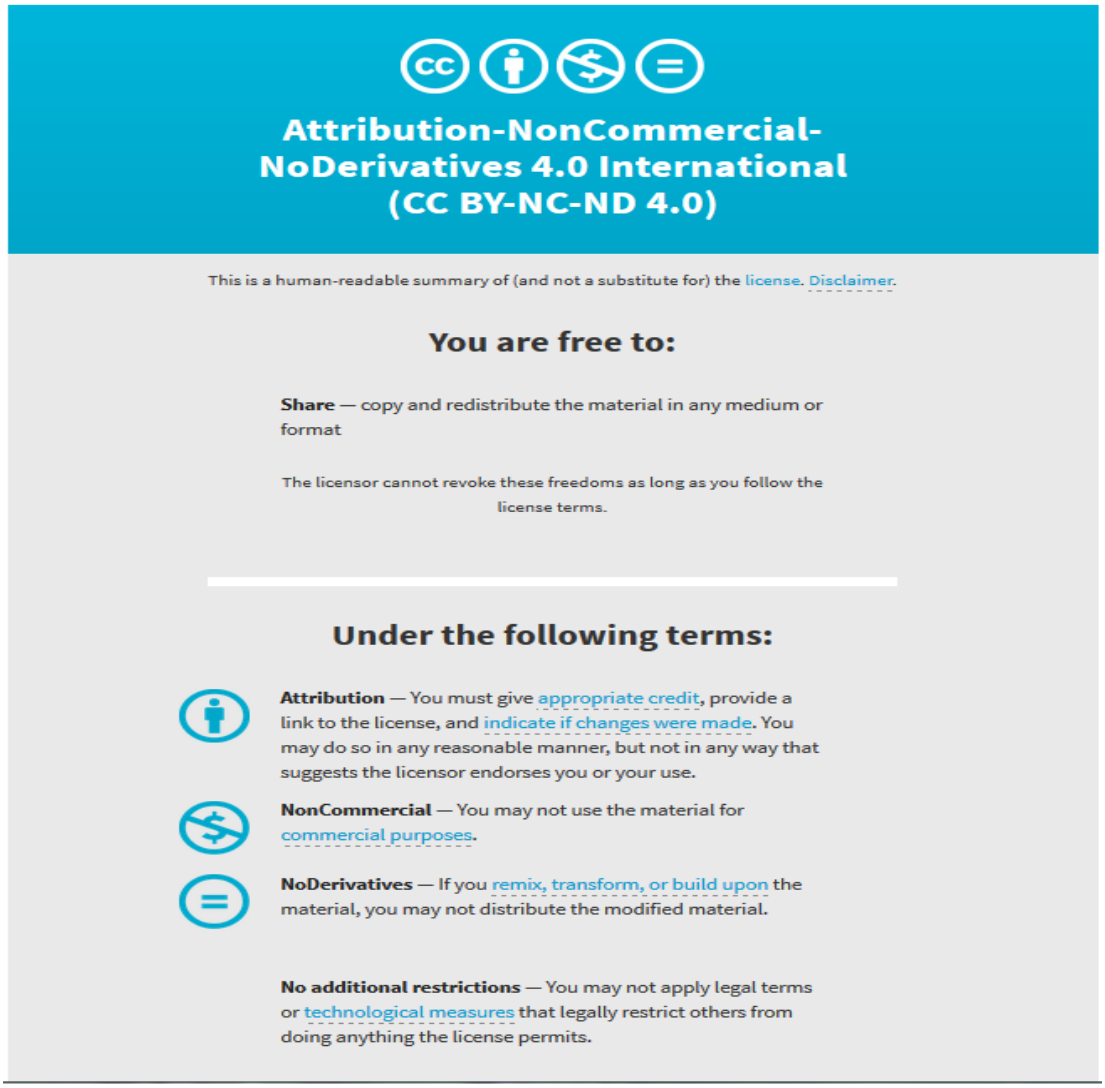

25 July 2017

Geoscience Frontiers 8 (2017) 1–14

HOSTED BY

Contents lists available at ScienceDirect

China University of Geosciences (Beijing)

Geoscience Frontiers

journal homepage: www.elsevier.com/locate/gsf

Research paper

Reappraising the *P–T* evolution of the Rogaland–Vest Agder Sector, southwestern Norway

Eleanore Blereau [a,*], Tim E. Johnson [a], Chris Clark [a], Richard J.M. Taylor [a], Peter D. Kinny [a], Martin Hand [b]

[a] Department of Applied Geology, The Institute for Geoscience Research (TIGeR), Curtin University, Perth 6845, Western Australia, Australia
[b] Centre for Tectonics, Resources and Exploration (TRaX), School of Earth and Environmental Sciences, University of Adelaide, Adelaide 5005, South Australia, Australia

ARTICLE INFO

Article history:
Received 14 April 2016
Received in revised form
12 July 2016
Accepted 16 July 2016
Available online 10 August 2016

Keywords:
UHT
Phase equilibria modelling
Rogaland Igneous Complex
THERMOCALC
Sveconorwegian Orogen

ABSTRACT

The Rogaland–Vest Agder Sector of southwestern Norway comprises high-grade metamorphic rocks intruded by voluminous plutonic bodies that include the ~1000 km^2 Rogaland Igneous Complex (RIC). New petrographic observations and thermodynamic phase equilibria modelling of three metapelitic samples collected at various distances (30 km, 10 km and ~10 m) from one of the main bodies of RIC anorthosite were undertaken to assess two alternative *P–T–t* models for the metamorphic evolution of the area. The results are consistent with a revised two-phase evolution. Regional metamorphism followed a clockwise *P–T* path reaching peak conditions of ~850–950 °C and ~7–8 kbar at ~1035 Ma followed by high-temperature decompression to ~5 kbar at ~950 Ma, and resulted in extensive anatexis and melt loss to produce highly residual rocks. Subsequent emplacement of the RIC at ~930 Ma caused regional-scale contact metamorphism that affected country rocks 10 km or more from their contact with the anorthosite. This thermal overprint is expressed in the sample proximal to the anorthosite by replacement of sillimanite by coarse intergrowths of cordierite plus spinel and growth of a second generation of garnet, and in the intermediate (10 km) sample by replacement of sapphirine by coarse intergrowths of cordierite, spinel and biotite. The formation of late biotite in the intermediate sample may suggest the rocks retained small quantities of melt produced by regional metamorphism and remained at temperatures above the solidus for up to 100 Ma. Our results are more consistent with an accretionary rather than a collisional model for the Sveconorwegian Orogen.

1. Introduction

The Rogaland–Vest Agder Sector of SW Norway is a metamorphic province dominated by high-grade gneisses and intrusive igneous rocks (Maijer et al., 1981; Tobi et al., 1985; Jansen and Tobi, 1987; Maijer, 1987). Together these rocks represent the core of the *ca*. 1200–900 Ma Sveconorwegian Orogen (Falkum and Petersen, 1980; Falkum, 1985). The intrusive rocks include the Rogaland Igneous Complex (RIC) that is exposed over ~1000 km^2 and comprised largely of three massif-type anorthosite plutons emplaced around 930 Ma (Schärer et al., 1996). Two contrasting tectonic models have been proposed to explain the evolution of the Sveconorwegian Orogen, one involving continent-continent collision (Bingen et al., 2008) and the other involving protracted subduction-accretion (Slagstad et al., 2013a,b; Coint et al., 2015; Roberts and Slagstad, 2015). Collisional models generally require long timescales for the rocks to reach high-grade metamorphism (Clark et al., 2011; Slagstad et al., 2013a,b), whereas in accretionary orogens such conditions may be attained much faster (Slagstad et al., 2013a,b; Coint et al., 2015). However, clockwise *P–T* paths are not diagnostic of either tectonic setting (Brown, 2007).

The role of the RIC in the metamorphic history of the gneisses of the Rogaland–Vest Agder Sector is controversial, and two different *P–T–t* models have been advanced (Fig. 3). Möller et al. (2003) and Tomkins et al. (2005) proposed a two-stage metamorphic evolution, in which an upper amphibolite facies regional event characterized by a clockwise *P–T* evolution was followed by ultra-high

* Corresponding author.
E-mail address: eleanore.blereau@postgrad.curtin.edu.au (E. Blereau).
Peer-review under responsibility of China University of Geosciences (Beijing).

http://dx.doi.org/10.1016/j.gsf.2016.07.003

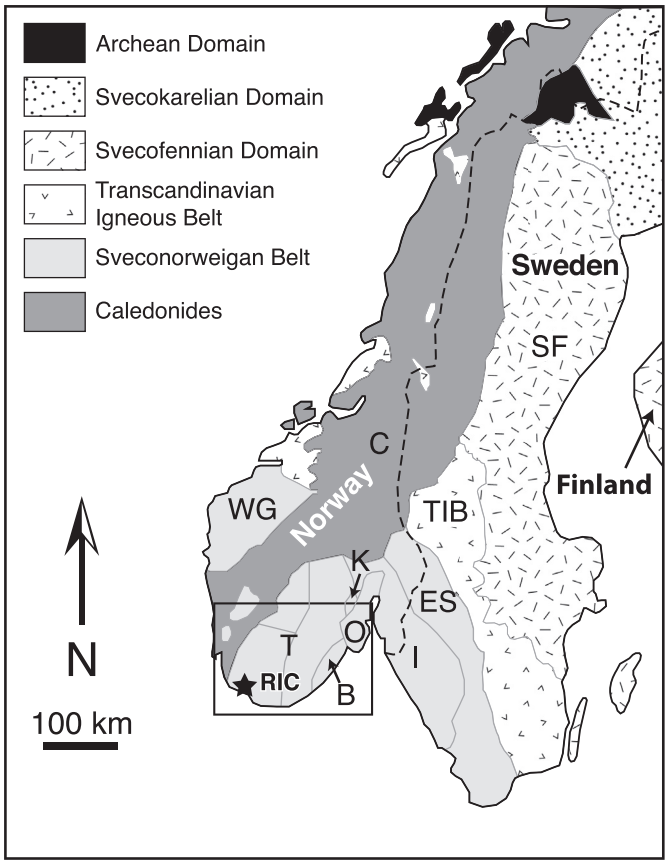

Figure 1. Map showing the main geological subdivisions of Scandinavia (after Bergh et al., 2012). Abbreviations: T – Telemarkia Terrane; B – Bamble Sector; O – Oslo Graben; K – Kongsberg Sector; I – Idefjorden Terrane; ES – Eastern Segment; C – Caledonides; TIB – Transcandinavian Igneous Belt; SF – Svecofennian Domain; WG – Western Gneiss Region.

temperature (UHT) metamorphism at lower pressure related to intrusion of the RIC. By contrast, Drüppel et al. (2013) proposed a single-stage, protracted clockwise regional metamorphic evolution that reached a UHT metamorphic peak some 70 Ma prior to emplacement of the RIC; in this model, high-grade metamorphism and intrusion are considered to have been unrelated.

In this study, we combine new petrographic observations with phase equilibria modelling of three metapelitic samples collected at different distances from the RIC (30 km, 10 km and <50 m) to re-evaluate their metamorphic evolution. We discuss the implications of the results for the tectonic evolution of the Sveconorwegian Belt.

2. Regional geology

The rocks of southern Scandinavia experienced three Proterozoic orogenic events: in Sweden and Finland the *ca.* 1900–1750 Ma Svecofennian orogeny, in SE Norway and Sweden the *ca.* 1750–1550 Ma Gothian orogeny, and in southern Norway and SW Sweden the *ca.* 1200–900 Ma Sveconorwegian orogeny (Andersen et al., 2002). The Sveconorwegian Belt lies to the west of the Svecofennian Domain and the *ca.* 1850–1650 Ma Transcandinavian Igneous Belt and is bounded obliquely to the northwest by the Caledonides (Fig. 1). It comprises a number of lithotectonic domains, including the Eastern Segment, Idefjorden Terrane, Bamble, Kongsberg and Telemarkia Terranes, all of which are bounded by major shear zones (Fig. 1). The Telemarkia Terrane is interpreted to have formed in a short magmatic event between 1520–1480 Ma (Bingen et al., 2005, 2006; Bogdanova et al., 2008; Roberts and Slagstad, 2015) and is further divided into the Telemark, Hardangervidda, Sudal and Rogaland–Vest Agder Sectors (Fig. 2).

The focus of this study, the Rogaland–Vest Agder (RVA) Sector, is a high-grade gneiss complex intruded by voluminous synorogenic plutons that represents the core of the Sveconorwegian Orogen (Falkum and Petersen, 1980; Falkum, 1985). The complex consists of felsic orthogneiss, much of which contains orthopyroxene, and subordinate garnet-bearing paragneiss (Hermans et al., 1975; Falkum, 1982, 1985; Tobi et al., 1985; Bingen et al., 2005; Tomkins et al., 2005; Coint et al., 2015), with minor amphibolite, quartzite, calc-silicate and marble (Huijsmans et al., 1981; Falkum, 1982, 1985; Tobi et al., 1985; Jansen and Tobi, 1987; Bingen et al., 2005; Harlov, 2011). The orthopyroxene-bearing orthogneiss is variably migmatitic, in which migmatised varieties have protolith ages of *ca.* 1450 Ma whereas non-migmatised varieties have younger protolith ages of *ca.* 1230–1210 Ma (Coint et al., 2015). Migmatitic garnet-bearing paragneiss contains abundant garnet as well as sillimanite and/or cordierite-bearing layers indicating pelitic to semi-pelitic protoliths (Hermans et al., 1975; Coint et al., 2015). Detrital zircon U–Pb ages between *ca.* 3000–1200 Ma have been reported from one of these migmatitic metapelites (Tomkins et al., 2005).

The RVA Sector contains three suites of intrusive rocks: (1) the Sirdal Magmatic Belt (SMB); (2) the hornblende-biotite granites (HBG) and (3) the Rogaland Igneous Complex (RIC). The 1060–1020 Ma SMB, which covers an aerial extent of ~10,000 km^2, is a weakly deformed calc-alkaline granitic batholith that preserves igneous textures (Slagstad et al., 2013a,b; Coint et al., 2015). The main constituent is porphyritic biotite granite with lesser amounts of leucogranite, garnet granite and zones rich in xenoliths including migmatitic gneiss (Coint et al., 2015). The arc-like compositions of the SMB (Slagstad et al., 2013a,b) may reflect characteristics inherited from the source rocks, which were probably *ca.* 1500 Ma calc-alkaline metavolcanics and granitoid rocks such as are common in southern Norway, in particular in the Telemark and Hardangervidda Sector (Coint et al., 2015).

The 990–932 Ma HBG suite occurs as discrete 'A-type' plutons that crop out across the Telemarkia Terrane (Bogaerts et al., 2003; Vander Auwera et al., 2011). The range in composition in the HBG Suite from gabbronorite to granite (50–77 wt.% SiO_2) is interpreted to reflect extreme fractional crystallization of several batches of basaltic magma (Bogaerts et al., 2003). The HBG suite was likely derived from an undepleted to slightly depleted hydrous mafic source that was underplated during a previous orogenic event (Bogaerts et al., 2003; Vander Auwera et al., 2011, 2014).

The ~1000 km^2 RIC, also referred to as the Rogaland Anorthosite Complex (Pasteels et al., 1979; Schärer et al., 1996; Bogaerts et al., 2003; Westphal et al., 2003) and Rogaland Anorthosite Province (Sauer et al., 2013; Coint et al., 2015), is composed of three massif-type anorthosites (Egersund-Ogna, Håland-Heleren and Åna-Sira) as well as a large layered polyphase intrusion (Bjerkreim-Sokndal lopolith), two smaller leuconorite bodies (Hidra and Garsaknatt) and a small number of mafic dykes (high-Al gabbros to orthopyroxene monzonorite) (Pasteels et al., 1979; Wilmart et al., 1991; Vander Auwera and Longhi, 1994; Nijland et al., 1996; Schärer et al., 1996; Duchesne and Wilmart, 1997; Bolle et al., 2002; Marker et al., 2003; Möller et al., 2003; Bolle et al., 2010). The three anorthosite massifs contain subophitic aggregates of megacrystic plagioclase and aluminous orthopyroxene within fine-grained leuconorite (Schärer et al., 1996; Bybee et al., 2014). U–Pb ages of zircon and baddeleyite inclusions within orthopyroxene megacrysts in the Egersund-Ogna, Håland-Heleren and Åna-Sira anorthosites are identical within uncertainty at *ca.* 930 Ma (Schärer

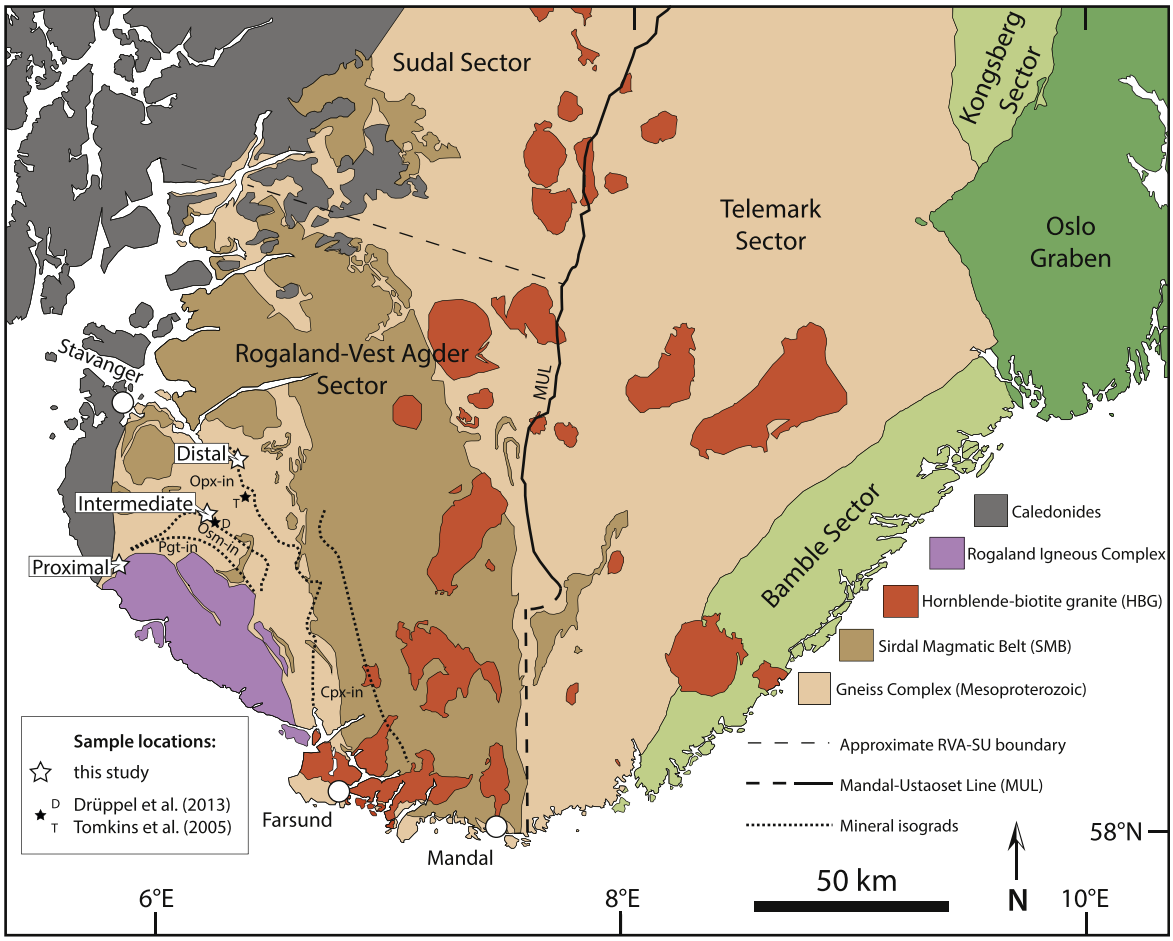

Figure 2. Geological map of the Rogaland–Vest Agder Sector of southwest Norway (after Coint et al. (2015), MUL from Vander Auwera et al. (2011) and mineral isograds from Bolle et al. (2010)). Samples from this study are marked as large white stars with locations from previous studies as smaller black stars.

et al., 1996). Based on the complex spread of zircon U–Pb ages reported by Möller et al. (2003), the RIC suggested by Coint et al. (2015) has a protracted, episodic emplacement history. The margin of the Egersund-Ogna massif has a magmatic foliation parallel to both its boundary and to the foliation of the adjacent host gneisses (Schärer et al., 1996; Bolle et al., 2002) that has been used as evidence for diapiric emplacement of a ~1150 °C crystal mush (Duchesne and Michot, 1987; Longhi et al., 1993; Schärer et al., 1996; Bolle et al., 2002). The anorthosites were emplaced at mid crustal depths (minimum of 5.0–7.7 kbar, ~20–30 km) based on conventional thermobarometry and numerical modelling (Wilmart and Duchesne, 1987; Barnichon et al., 1999).

Within the RIC, the Bjerkreim-Sokndal lopolith is a layered intrusion with four main phases; a basal phase of anorthosite–leuconorite and norite with rhythmic layering is overlain by monzonorite that is in turn overlain by monzonite and, lastly, by quartz monzonite (Versteeve, 1975; Wilmart et al., 1991; Duchesne and Wilmart, 1997; Bolle et al., 2002). The lopolith, which is separated from the anorthosite intrusions by a thin septum of gneissic country rocks, was emplaced at approximately the same time (Wilmart et al., 1991; Vander Auwera and Longhi, 1994; Schärer et al., 1996; Duchesne and Wilmart, 1997). Geochemical and isotopic data indicate that the RIC had a relatively anhydrous, lower crustal source (Bogaerts et al., 2003) with more recent studies suggesting that the parent magmas originated at the Moho with anorthosite formation tied to protracted magmatism in a convergent arc (Bybee et al., 2014). Previous studies suggested multiple parental melt compositions for the RIC suite, with source rocks possibly ranging from high Al-basalt to primitive orthopyroxene monzonorite (Vander Auwera et al., 2011, and references therein).

The high-grade gneisses of the RVA Sector are considered by some authors to have experienced a polymetamorphic evolution, and to preserve textural evidence for a regional metamorphic event followed by a high temperature contact metamorphic overprint (Verschure et al., 1980; Maijer et al., 1981; Wielens et al., 1981; Demaiffe and Michot, 1985; Jansen et al., 1985; Tobi et al., 1985; Maijer, 1987; Bingen and van Breemen, 1998; Möller et al., 2003; Tomkins et al., 2005; Coint et al., 2015). Evidence for an amphibolite facies regional metamorphic event (commonly termed M_1) at *ca.* 1035 Ma (Tomkins et al., 2005) is based on isotopic data from a garnet–biotite–sillimanite metapelite, ~25–30 km from the contact with the RIC (Möller et al., 2003). Coint et al. (2015) also suggested a similar age of regional metamorphism of *ca.* 1030 Ma. The subsequent growth in this rock of cordierite containing zircon dated at *ca.* 955 Ma indicates that peak metamorphic conditions were followed by decompression (shown in red, Fig. 3) (Möller et al., 2003; Tomkins et al., 2005). These events predate the emplacement of the RIC at *ca.* 930 Ma (Schärer et al., 1996), which caused large-scale contact metamorphism (M_2) at UHT conditions (shown in blue, Fig. 3) (Schärer et al., 1996; Möller et al., 2003; Westphal et al., 2003). Pressure–temperature estimates of ~750 °C at 5–7 kbar for the regional event and 700–1050 °C at ~4 kbar for the contact metamorphism were derived using

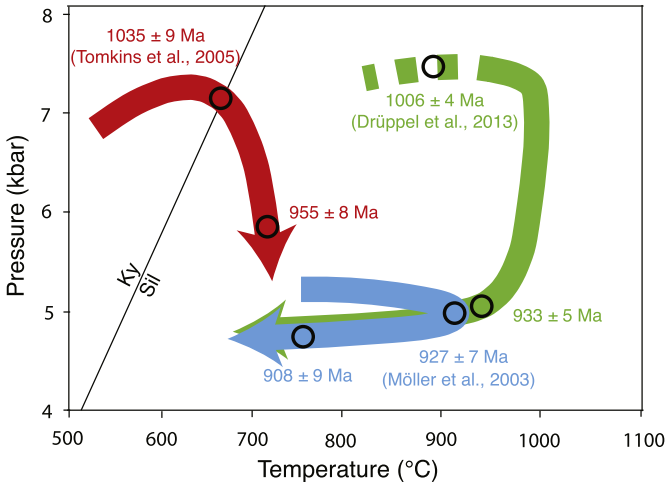

Figure 3. Two alternative *P–T* models proposed for the Rogaland–Vest Agder sector (modified after Drüppel et al., 2013); two-stage metamorphic evolution (Möller et al., 2003; Tomkins et al., 2005) versus protracted, single-stage metamorphic evolution (Drüppel et al., 2013).

conventional thermobarometry (Jansen et al., 1985). A later retrograde overprint (so-called M_3) to upper amphibolite to granulite facies at 908 Ma (550–700 °C and 3–5 kbar) is interpreted to be related to the isobaric cooling of intrusive bodies with the partial replacement of high grade minerals such as osumilite (Kars et al., 1980; Maijer et al., 1981; Wielens et al., 1981; Jansen et al., 1985; Bol et al., 1989; Nijland et al., 1996; Möller et al., 2003; Tomkins et al., 2005; Bolle et al., 2010).

In contrast to the previous interpretations, Drüppel et al. (2013) reinterpreted the gneisses as having experienced a single, long-lived regional metamorphic event that peaked at UHT conditions some 70 Ma prior to intrusion of the RIC (shown in green, Fig. 3). This interpretation, based on phase equilibria modelling in the Na_2O–CaO–K_2O–FeO–MgO–Al_2O_3–SiO_2–H_2O–TiO_2 (NCKFMASHT) model system of samples ~10 km from the RIC contact, indicated peak conditions of ~1000 °C at ~7.5 kbar were followed by near isothermal decompression to <5.5 kbar at 900–1000 °C (M_2) before near isobaric cooling (Drüppel et al., 2013). These authors concluded that no second thermal pulse is recorded by the silicate mineral assemblage in the RVA Sector. Zircon U–Pb ages are consistent with a metamorphic age at *ca.* 1000 Ma; epitaxial xenotime yields U–Pb ages within error of the emplacement of the RIC at *ca.* 930 Ma (Drüppel et al., 2013).

A series of high-*T* mineral-in isograds, including inverted pigeonite in felsic orthogneiss, osumilite in paragneiss, orthopyroxene in felsic orthogneiss and clinopyroxene in granodioritic gneiss, are broadly parallel to the margin of the RIC (Fig. 2) (Hermans et al., 1975; Pasteels et al., 1979; Sauter, 1981; Jansen et al., 1985; Tobi et al., 1985; Maijer, 1987; Bol et al., 1989). These isograds represent a temperature range from ~700 °C at the orthopyroxene-in isograd to over 900 °C (UHT) at the pigeonite-in isograd (Jansen et al., 1985; Tobi et al., 1985; Bol et al., 1989; Möller et al., 2002, 2003; Tomkins et al., 2005). Whereas most studies have interpreted the osumilite and pigeonite-in isograds as the products of contact metamorphism at *ca.* 930 Ma superimposed upon granulite to amphibolite-facies regional metamorphic assemblages, others regard the orthopyroxene isograd to pre-date the contact event (Bingen and van Breemen, 1998), More recently, Coint et al. (2015) have proposed that the orthopyroxene-in isograd separates granulite-facies rocks to the west from non-metamorphosed granites to the east and should not be regarded as an isograd at all.

3. Sample descriptions and petrology

Three samples collected from different distances from the RIC–country rock contact were investigated in order to evaluate their metamorphic histories. Hereafter, these samples are referred to as distal (collected ~30 km from the RIC), intermediate (~10 km) and proximal (~10 m), as shown in Fig. 2. Mineral abbreviations follow Kretz (1983) and Whitney and Evans (2010).

3.1. Distal sample (N58°49′49.4″, E6°16′49.2″)

The distal sample (ROG13/11) is a garnet–sillimanite–cordierite metapelite collected a short distance up-grade of the orthopyroxene-in isograd. The sample site, ~400 m NW of Giljastølsvatnet, is ~5 km north of the sample locality of Degeling et al. (2001) and Tomkins et al. (2005) (Fig. 2). The sample is a migmatite comprising melanosome rich in garnet, sillimanite and cordierite and garnet-bearing leucosomes that are continuous at an outcrop scale and oriented sub-parallel to the regional foliation (Fig. 4a).

In thin section, the melanosome contains anhedral garnet porphyroblasts (2–8 mm) within which abundant inclusions of sillimanite define a folded foliation that curves into parallelism with the matrix foliation (Fig. 4b, c) that is also defined by sillimanite (0.2–1 mm). Variably pinitised cordierite (2–6 mm, 10–15%) surrounds garnet, sillimanite, ilmenite and quartz (Fig. 4b, c). Minor feldspar is also present within the matrix. Minor singular grains of ilmenite (0.5–1 mm) are partially to completely replaced by intergrowths of differently orientated rutile and chlorite. The leucosome is composed of sub-equal proportions of quartz (2–6 mm), plagioclase (1–4 mm) and K-feldspar (2–4 mm), along with anhedral to rounded garnet (1–3 mm) that contains abundant inclusions of quartz but no sillimanite (Fig. 4d). Minor biotite is present (0.5–1 mm) along with small amounts of muscovite.

The interpreted peak assemblage in sample ROG13/11 is garnet, sillimanite, plagioclase, K-feldspar, quartz, ilmenite and melt. Matrix garnet containing sillimanite inclusions is interpreted to mainly represent subsolidus growth, whereas leucosome garnet that lacks sillimanite inclusions is regarded as a peritectic product of melting reactions consuming biotite. Cordierite and biotite are considered to be retrograde minerals.

3.2. Intermediate sample (N58°42′9.7″, E6°10′1.4″)

The intermediate sample (ROG13/10) is a residual sapphirine-bearing metapelite from a locality near Ivesdal, ~10 km NE of the RIC contact (Fig. 2), which has been described previously by Hermans et al. (1976) and Drüppel et al. (2013). The exposure consists of irregular, dark sapphirine-bearing layers within a host orthopyroxene-bearing gneiss (Fig. 5). Minor and sporadically dispersed large garnets (~3–8 cm) within the sapphirine-bearing granulite and, less commonly, within the orthopyroxene gneiss have coronae of orthopyroxene with or without plagioclase, and in some cases have been replaced completely (Fig. 5a, b). Garnet-bearing leucosome occurs as rare patches within orthopyroxene gneiss. Sparse quartz veins occur within, and cross-cut both lithologies. Irregular orthopyroxene-rich selvedges and schlieren occur within the orthopyroxene gneiss and occasionally along contacts between orthopyroxene gneiss and sapphirine-bearing metapelite.

In thin section, subhedral to euhedral sapphirine porphyroblasts (1–8 mm, 10–15%) are partially to completely replaced by coarse intergrowths of spinel and cordierite, along with variable amounts of biotite that appears to be replacing cordierite (Fig. 6a, b, d). The matrix consists of cordierite (0.5–3 mm), orthopyroxene

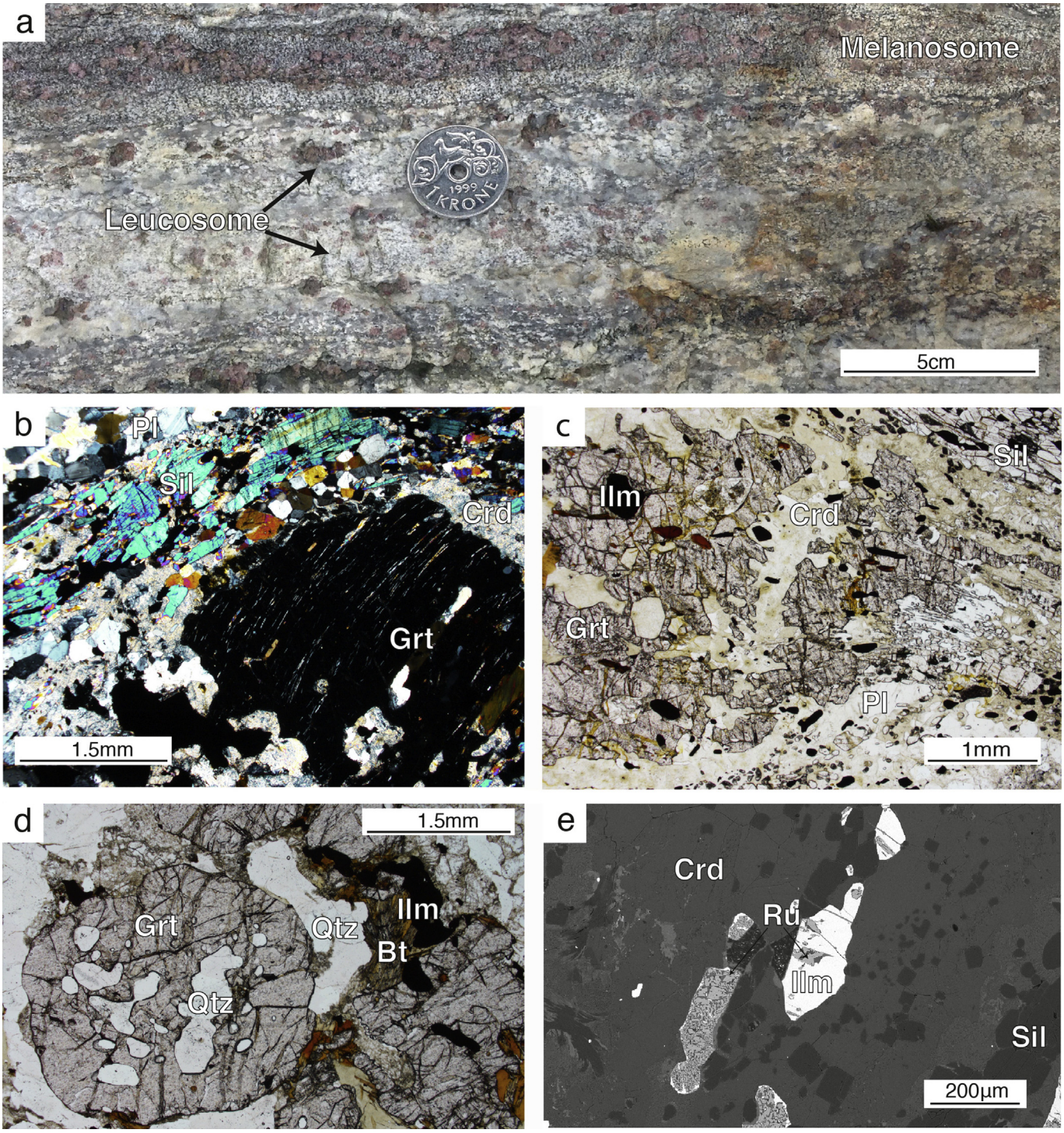

Figure 4. Field photograph and photomicrographs from the 'Distal' locality. (a) Garnet–cordierite–sillimanite melanosome with garnet-bearing leucosome at outcrop scale. (b) Garnet porphyroblast within melanosome (xpl) containing ilmenite, sillimanite and minor biotite inclusions, surrounded by pinitised cordierite and sillimanite. (c) Garnet porphyroblast within melanosome with sillimanite inclusions defining a relict foliation. Coarse sillimanite in the matrix defines a new foliation. (d) Peritectic garnet with quartz inclusions within leucosome, with late biotite. (e) Back scattered electron (BSE) image showing ilmenite being replaced by an intergrowth of rutile and chlorite within the melanosome.

(0.5–3 mm), plagioclase (0.5–2 mm), K-feldspar (0.5–1 mm) and biotite (up to 2 mm) (Fig. 6c). Orthopyroxene grains are separated from sapphirine porphyroblasts by layers of cordierite and spinel plus cordierite (Fig. 6a, b). Feldspar grains are variably sericitised. Spinel contains ilmenite and minor exsolved magnetite. Quartz is absent.

We interpret sample ROG13/10 to have contained an earlier assemblage of sapphirine, orthopyroxene, plagioclase, K-feldspar, cordierite, ilmenite and melt that later underwent replacement of sapphirine and orthopyroxene by coarse intergrowths of spinel and cordierite. Subsequent growth of biotite may reflect retrograde reaction in the presence of melt.

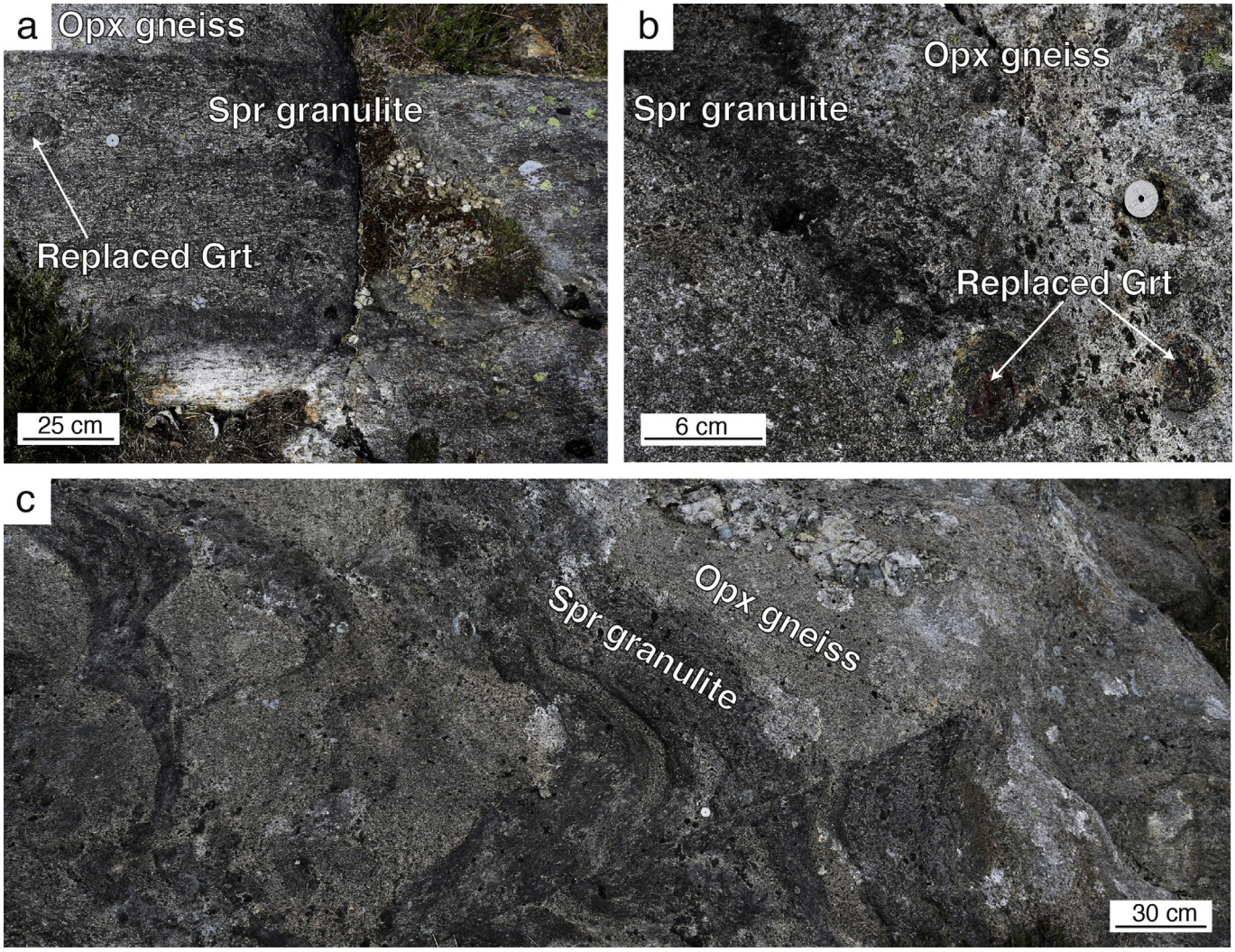

Figure 5. Field photographs from the 'Intermediate' locality. (a) Dark sapphirine granulite layer with completely replaced garnet. (b) Sapphirine granulite and orthopyroxene gneiss containing partially replaced garnets with orthopyroxene coronas. (c) Irregular dark layers of sapphirine granulite interleaved with orthopyroxene gneiss, cut by minor faults.

3.3. Proximal sample (N58°35′46.5″, E5°46′59.0″)

The proximal sample ROG14/5 is from country rocks ~10 m from the northwest margin of the RIC (Fig. 2). The sample is a migmatitic garnet–sillimanite–spinel–cordierite metapelitic gneiss (Fig. 7a) that is intruded by several small sheets of garnet-bearing anorthosite (Fig. 7b). The metapelite consists of melanosome rich in garnet and cordierite, within which occurs narrow, foliation-parallel leucosome layers (<1 cm in width). Larger (~0.5–1 m) irregular bodies of garnet-bearing and garnet-free leucosome cross-cut the foliation and contain schollen of melanosome (Fig. 7a). Minor quartz veins are also present. The anorthosite sheets are discontinuous, up to 15 cm wide and 4 m in length and oriented parallel to the foliation (Fig. 7b).

In thin section, sample ROG14/5 is dominated by melanosome containing equant to elongate anhedral garnet porphyroblasts (0.5–4 mm) containing sillimanite inclusions (Fig. 7c, d). A second generation of garnet forms narrow (~100 μm) rims around pre-existing garnet porphyroblasts and adjacent to spinel (Fig. 7c, d). Coarse matrix sillimanite (0.5–4 mm) defines a foliation that wraps around garnet, and is partially replaced by intergrowths of spinel plus cordierite (Fig. 7d). Spinel occurs both within the symplectite and as aggregates of grains surrounded by a thin rind of cordierite or garnet (Fig. 7d). The leucosome contains large (2–8 mm) slightly elongate grains along with smaller (0.5–2 mm) grains of quartz, plagioclase (1–2 mm) and K-feldspar (1–2 mm). Cordierite surrounds garnet, sillimanite and, less commonly, quartz and spinel (1–2 mm) and is sometimes intergrown with K–feldspar (Fig. 7d). Minor ilmenite is partially to completely replaced by late intergrowths of rutile and chlorite.

This sample is interpreted to contain an earlier assemblage of garnet, sillimanite, plagioclase, K-feldspar, quartz, spinel, ilmenite and melt. Replacement of sillimanite by cordierite plus spinel, and growth of a second generation of garnet occurred subsequently.

4. Phase equilibria modelling

Metamorphic *P–T* conditions were constrained using *P–T*, *P–X* and *T–X* pseudosections modelled in the Na_2O–CaO–K_2O–FeO–MgO–Al_2O_3–SiO_2–H_2O–TiO_2–O system using THERMOCALC 3.40i and the internally consistent thermodynamic dataset of Holland and Powell (2011) (specifically the tc-ds62 dataset generated on 06/02/2014). Activity–composition models are from White et al. (2014a). Although Mn-bearing solution models have been

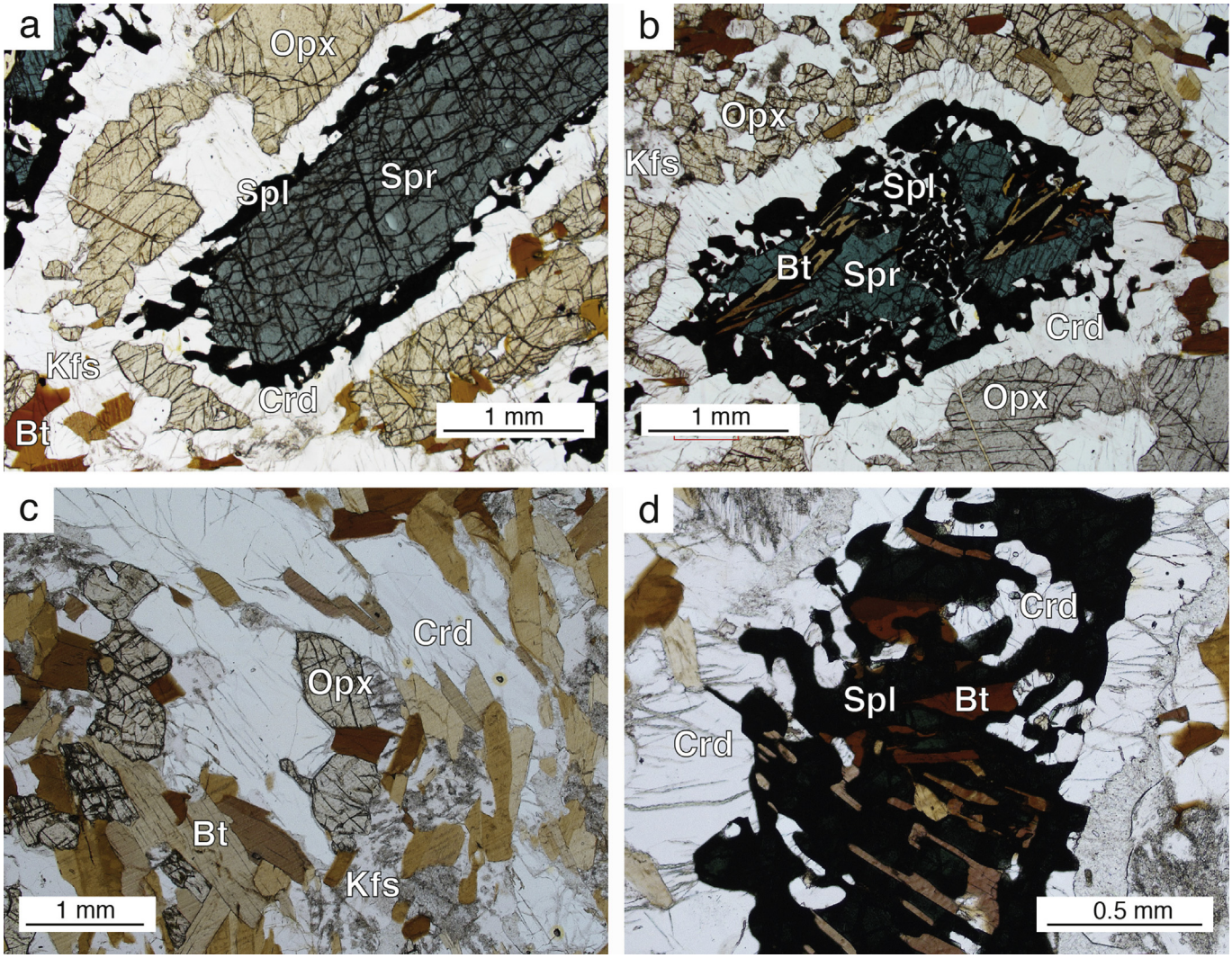

Figure 6. Photomicrographs from the 'Intermediate' locality. (a) Sapphirine porphyroblast rimmed by spinel plus cordierite and a cordierite rim separating the symplectite from orthopyroxene. (b) Sapphirine partially replaced by a spinel–cordierite symplectite, with later biotite replacing cordierite within the symplectite. An outer rim of cordierite is present between the symplectite and orthopyroxene. (c) Irregular grains of orthopyroxene and cordierite within the matrix with some grains almost completely surrounded by late biotite. (d) Spinel plus cordierite symplectite with biotite partially replacing cordierite.

calibrated (White et al., 2014b), Mn has a negligible effect at high temperatures and was not considered (Johnson et al., 2015). Calculations consider the phases garnet, silicate melt, plagioclase, K-feldspar, sillimanite, sapphirine, quartz, muscovite, biotite, orthopyroxene, cordierite, ilmenite, rutile and magnetite-spinel. Osumilite was not included as there is no solution model calibrated against the ds6 dataset.

Bulk rock compositions were determined by X-ray fluorescence analysis using a Panalytical 2404 XRF unit at Franklin and Marshall College, Pennsylvania, for which ferric and ferrous iron contents were determined by titration. The bulk compositions (expressed as mol.% oxides) used in the pseudosections are given in Table 1. Modelled H_2O contents were constrained using *T–X* or *P–X* pseudosections ranging from a quantity assuming all analysed loss on ignition (LOI) as H_2O to lower values (0.1 mol.%). The H_2O content chosen for *P–T* modelling was such that the solidus intersected, or was as close as possible to the field containing the interpreted peak assemblage (see Supplementary data Figs. S1–3). Calculations using the composition of the distal sample (ROG13/11), the most altered of the studied rocks, measured ferric iron concentrations were too high with all calculated fields containing magnetite, which is not observed in the rock. Thus, to account for post-peak oxidation, appropriate ferric iron contents were constrained using a *P–X* pseudosection ranging from the titrated value (1.31 mol.% Fe_2O_3) to a minimal content (0.01 mol.%; see Supplementary data Fig. S4). A value of X = 0.5 (Fe_2O_3 = O = 0.67 mol.%) was chosen, as it is the minimum required to eliminate magnetite from the interpreted peak assemblage. Note that the stability field of spinel in nature is likely to be larger than the calculated stability due to the presence of minor components (e.g. Zn, V, Cr) that cannot currently be modelled (Tajčmanová et al., 2009). Drüppel et al. (2013) reported average concentrations of Cr_2O_3 and ZnO in spinel in the sapphirine-bearing sample as 0.07 and 0.15 wt.%, respectively. For reference, *P–T* pseudosections contoured for the abundance of particular phases calculated using TCInvestigator (Pearce et al., 2015) are given in the Supplementary data (Fig. S5).

4.1. Distal sample

In the *P–T* pseudosection for sample ROG13/11 (Fig. 8), the solidus for the chosen H_2O content is located at ~830 °C at pressures above 7 kbar. Between 6–7 kbar the solidus inflects to higher

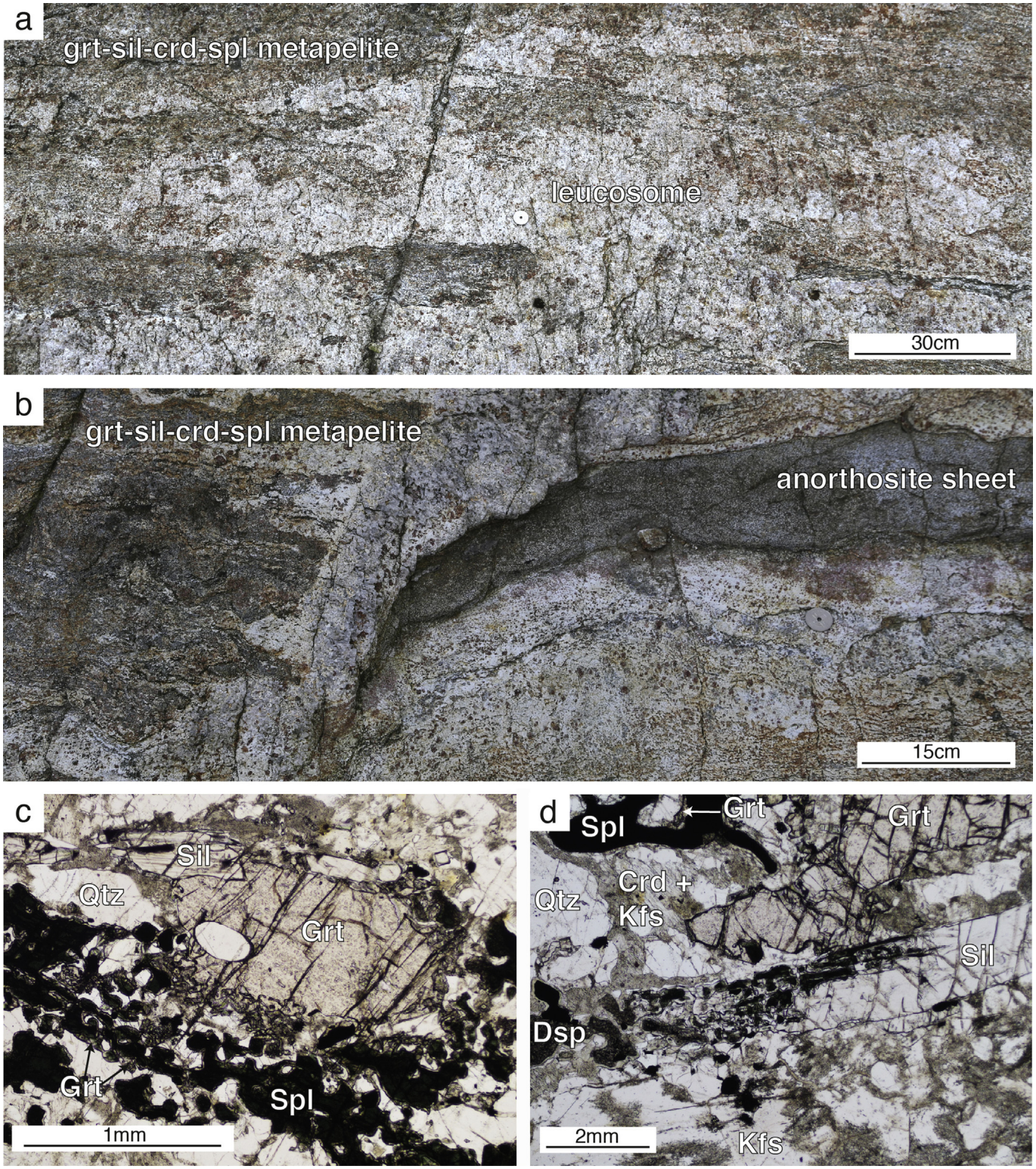

Figure 7. Field photographs and photomicrographs from the 'Proximal' locality. (a) Garnet–sillimanite–cordierite–spinel migmatite overprinted by a large irregular garnet-bearing leucosome containing schollen of the metapelite. (b) Metapelite with intruded anorthosite sheet. (c) Garnet porphyroblast with secondary garnet overgrowing spinel. (d) Sillimanite partly replaced by spinel plus cordierite, with some of the spinel replaced by diaspore.

temperatures (~970 °C) due to the presence of cordierite that partitions some of the H_2O that at higher pressures is contained within melt. For the chosen ferric iron content and *P*–*T* range, ilmenite is stable throughout and magnetite is predicted only at low temperatures and pressures. The interpreted peak assemblage of garnet, sillimanite, plagioclase, K-feldspar, quartz, ilmenite and melt occupies a large stability field at >850 °C and >6 kbar (outlined in red, Fig. 8). At lower temperatures biotite is stable, and at lower pressures cordierite, which occurs replacing garnet at its margins, is predicted. The calculated stability fields of spinel and

Table 1
Bulk compositions as molar oxide (mol.%) used in phase equilibria modelling.

Sample	SiO_2	TiO_2	Al_2O_3	O	FeO	MgO	CaO	Na_2O	K_2O	H_2O	Total
ROG13/11 (Distal)	68.95	0.78	12.95	0.67	6.86	3.68	1.39	1.82	2.80	0.10	100
ROG13/10 (Intermediate)	51.45	0.64	14.98	1.13	6.73	17.99	1.33	1.78	2.94	1.03	100
ROG14/5 (Proximal)	63.19	0.83	16.71	0.57	9.29	4.85	1.28	1.11	2.06	0.11	100

orthopyroxene occur at higher temperatures and lower pressures than the inferred peak, respectively.

4.2. Intermediate sample

In the *P–T* pseudosection for sample ROG13/10 (Fig. 9) the solidus for the chosen H_2O content is located at ~900–950 °C. The stability field for the interpreted earlier assemblage of sapphirine, orthopyroxene, plagioclase, K-feldspar, cordierite, ilmenite and melt is relatively narrow (in *T*) between 910–980 °C and between 4 and 8 kbar (outlined in red, Fig. 9). Cordierite is consumed at higher *T* and biotite is predicted at lower *T*, and garnet is stable at higher *P* and spinel at lower *P*. Compositional isopleths of Al–in–orthopyroxene are shown in Fig. 9. Maximum measured values of *X*(Al) (Al cations in the formula unit based on six oxygens) from samples from this locality are 0.18 according to Drüppel et al. (2013), and this isopleth, along with the one sigma uncertainty on its position, is shown as the shaded field. The measured Al content in orthopyroxene is consistent with the higher pressure part of the preferred peak field, implying peak conditions of around 7–8 kbar and 900–950 °C (Fig. 9). The subsequent evolution of the rock, expressed by the growth of cordierite, spinel and biotite at the expense of sapphirine, requires significantly lower pressures but similar temperatures that was followed by cooling into fields containing biotite.

4.3. Proximal sample

In the *P–T* pseudosection for proximal sample ROG14/5 (Fig. 10), the solidus for the chosen H_2O content is located at ~815 °C above 6.3 kbar but inflects to higher temperatures (~950–975 °C) below 6 kbar due to the presence of cordierite which partitions some of the H_2O that, at higher pressures, is contained within melt. The interpreted earlier assemblage of garnet, sillimanite, plagioclase, K-feldspar, quartz, ilmenite and melt but without spinel, defines a large stability field at 820 to >1000 °C and ~6 to >10 kbar (outlined in red, Fig. 10); spinel is predicted to become stable at higher temperatures. As spinel may be stabilised by non-system components, our preferred interpretation is that the earlier assemblage is consistent with the high *T* end of the modelled spinel-absent field or with the field containing spinel (i.e. >900 °C and >6 kbar). The subsequent evolution of this sample, indicated by the replacement of sillimanite by cordierite and spinel and the growth of a second generation of garnet and cordierite (shown by the arrow in Fig. 10), require lower pressures (~5–6 kbar) but similar temperatures.

5. Discussion

5.1. P–T conditions of regional metamorphism

At a distance of ~30 km from the contact, the distal sample is considered to be beyond the effects of contact metamorphism associated with the emplacement of the RIC and to preserve the regional metamorphic history. This is supported by a pronounced regional foliation and the lack of symplectitic replacement of porphyroblast phases that characterises the other samples. Petrographic observations coupled with phase equilibria modelling suggest that this sample experienced a clockwise regional *P–T* path, reaching peak conditions of >850 °C at >6 kbar. Partial replacement of garnet by cordierite implies high-temperature decompression to conditions of ~850 °C at 5 kbar, while the growth of biotite implies crystallisation of the last vestiges of melt upon cooling. A *P–T* path consistent with these observations is shown in Fig. 8. Peak conditions are poorly constrained due to the size and the calculated compositional and modal homogeneity of the phases within the inferred peak field. The high temperature subsolidus prograde path is constrained to the sillimanite field, with no evidence for the former presence of kyanite.

The inferred early assemblages developed within the intermediate sample (sapphirine, orthopyroxene, plagioclase, K-feldspar, cordierite, ilmenite and melt) and the proximal sample (garnet, sillimanite plagioclase, K-feldspar, quartz, ilmenite, spinel and melt), are similarly consistent with growth during regional metamorphism. Modelling of these compositions gives *P–T* conditions that are similar to those derived for the distal sample, namely 900–950 °C and ~7–8 kbar for the intermediate sample (Fig. 9) and >900 °C and >6 kbar for the proximal sample (Fig. 10). Clearly,

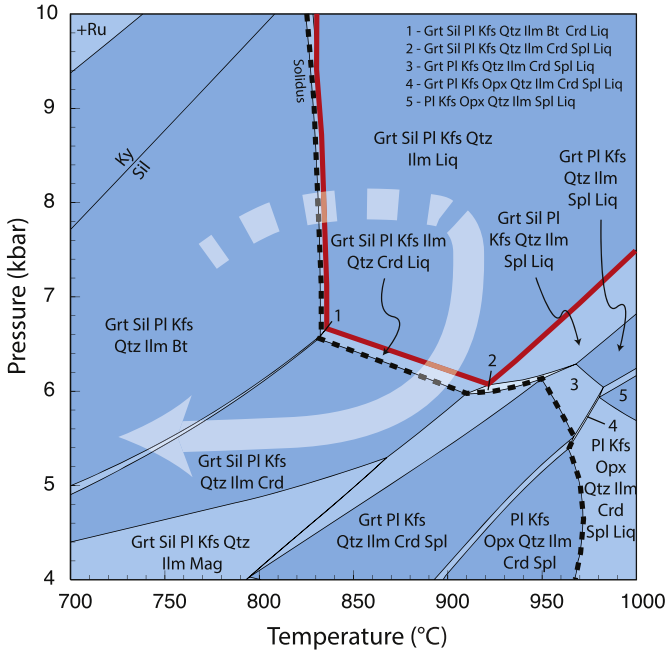

Figure 8. Modelled *P–T* pseudosection of the distal sample (ROG13/11) with peak field outlined in red and solidus marked by a black dashed line. The interpreted, clockwise *P–T* path traces the post-peak growth of cordierite and biotite. Positioning of the *P–T* path is based on modal isopleths generated using TCInvestigator (Pearce et al., 2015).

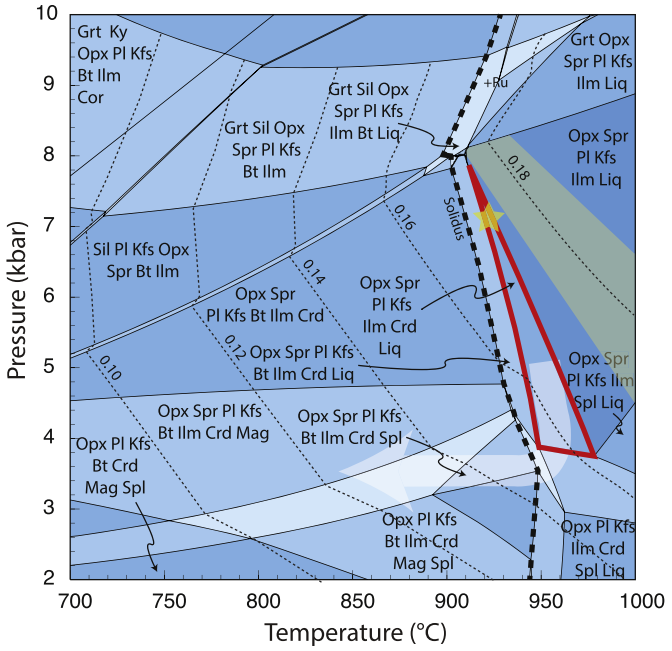

Figure 9. Modelled *P–T* pseudosection of the intermediate sample (ROG13/10) with peak field outlined in red, solidus marked by a black dashed line and y(opx) isopleths marked by fine dashed lines labelled with their respective values. Grey shaded area indicates uncertainty on the y(opx) = 0.18 isopleth. The presence of garnet defines the upper pressure limit of the peak assemblage, while cordierite defines the lower temperature limit. The star indicates the interpreted peak conditions reached during regional metamorphism. The illustrated portion of the *P–T* path traces the growth of spinel and cordierite and later biotite. Positioning of the *P–T* path is based on modal isopleths generated using TCInvestigator (Pearce et al., 2015).

all three samples cannot have followed an identical regional *P–T* path. However, we propose that a generalised, clockwise regional metamorphic evolution was experienced by all samples, which attained peak conditions of around 850–950 °C at 7–8 kbar, and

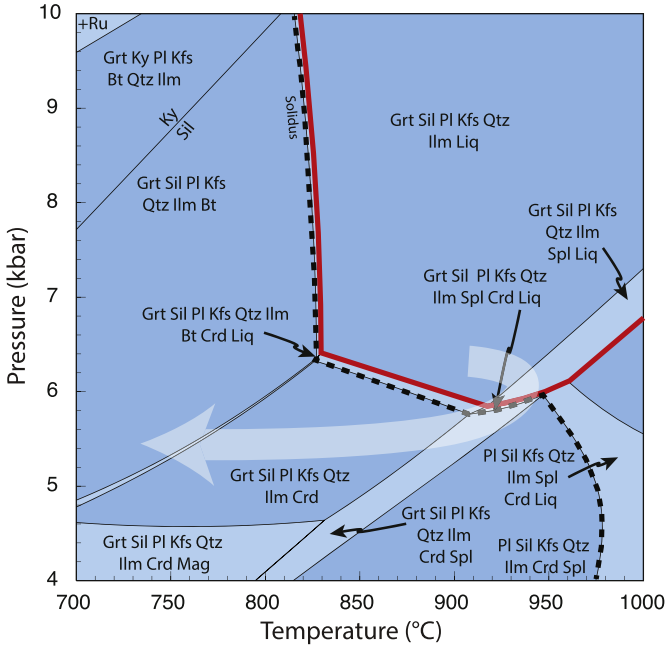

Figure 10. Modelled *P–T* pseudosection of the proximal sample (ROG14/5) with peak field outline in red and solidus marked by a black dashed line. The interpreted *P–T* path traces the growth of spinel, cordierite and secondary garnet.

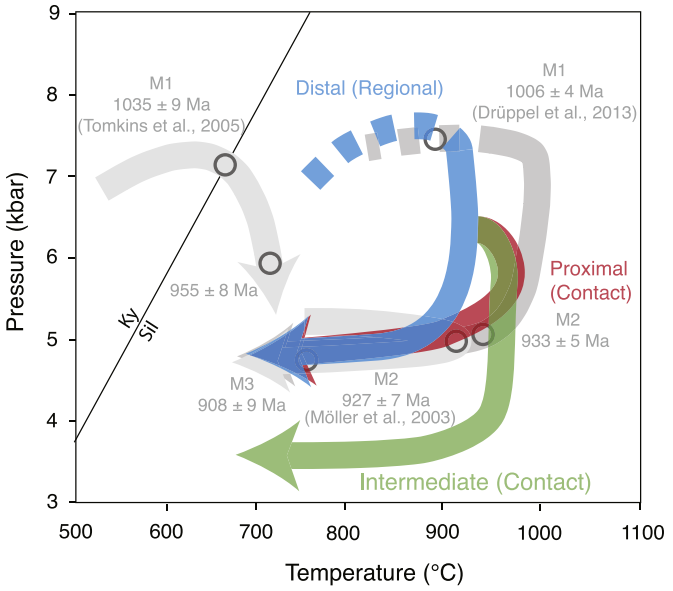

Figure 11. Summary diagram of the revised *P–T* evolution of the RVA Sector, with previous models in grey. Interpreted *P–T* evolution for the distal (blue), intermediate (green) and proximal (red) samples. The dashed approximate prograde evolution is based on the lack of kyanite in all samples.

was followed by high-temperature decompression to ~5 kbar, followed by near isobaric cooling (Fig. 8). Under such conditions, pelitic and greywacke protoliths will produce significant quantities of melt (Johnson et al., 2008; White et al., 2014a), most of which will have been lost to higher crustal levels to leave low $a(H_2O)$ granulite facies residua, consistent with observation.

Clockwise regional *P–T* paths were proposed by both Tomkins et al. (2005) and Drüppel et al. (2013). However, our inferred regional peak conditions are at least ~200 °C higher than those reported by Tomkins et al. (2005) based on conventional thermobarometry, and ~50 °C lower than the UHT regional conditions proposed by Drüppel et al. (2013), based on phase equilibria modelling (Fig. 11). Possible reasons for these differences are detailed below.

5.2. *P–T* conditions of contact metamorphism

Petrographic observations of the intermediate and proximal samples in conjunction with phase equilibria modelling suggest a two-stage evolution which we equate to: (1) high- to ultra-high *T* regional metamorphism with associated partial melting and melt loss (detailed above); and (2) subsequent high- to ultra-high *T* contact metamorphism of the residual rocks caused by emplacement of the RIC.

Importantly, the distal and proximal samples have strikingly similar bulk compositions, confirmed by the similarity in the *P–T* pseudosections for each (see Figs. 8 and 10). However, the petrographic features of the rocks are very different. Both are inferred to have had a regional peak assemblage containing garnet, sillimanite, plagioclase, K-feldspar, quartz, ilmenite, and melt, with the proximal sample inferred to have additionally contained a small quantity of spinel. However, the proximal sample contains a second generation of garnet (and spinel) that is lacking from the distal sample. In addition, sillimanite in the proximal sample is extensively replaced by a coarse intergrowth of cordierite plus spinel, whereas sillimanite in the distal sample is pristine. We interpret the coarse intergrowths of cordierite and spinel after sapphirine in the intermediate sample and after sillimanite in the proximal sample as

prograde reaction products that formed as a result of heating associated with emplacement of the RIC. Similar prograde reaction textures have been described elsewhere (Pitra and Waal, 2001; White et al., 2002; Johnson et al., 2004).

In the proximal sample, the reaction textures are consistent with contact metamorphic conditions of ~950 °C at ~5 kbar (Figs. 10 and 11). In the intermediate sample, the reaction textures are consistent with temperatures of ~950 °C and lower pressures of ~3–4 kbar (Figs. 9 and 11). The lower pressures inferred for the intermediate sample suggests it was at higher levels in the crust when the RIC was emplaced and implies tilting of the section and/or differential uplift and erosion post intrusion of the RIC. Overall, the pressures inferred for the contact metamorphism (3–6 kbar, Fig. 11) are similar to those reported by other authors (Möller et al., 2003; Tomkins et al., 2005). The high temperatures inferred for the contact metamorphism in the intermediate sample may suggest the anorthosite sits at shallow levels beneath these rocks. However, with no borehole data, the similarity in density between the anorthosite and host gneisses makes this difficult to test using geophysical means.

Within the intermediate sample, the growth of biotite replacing cordierite in the spinel-cordierite symplectites, which are themselves replacing sapphirine, suggests that the rocks may have retained small quantities of melt and that, on cooling and exhumation from the regional peak, the intermediate sample did not cross the solidus before the onset of contact metamorphism. This could indicate that the rocks stayed at high temperature for 100 Ma or more.

Our interpretation that the intermediate and proximal samples followed a two-stage *P–T* evolution (Fig. 11), with contact metamorphism superimposed upon the regional metamorphic evolution path, differs from the work of Drüppel et al. (2013). These authors suggest the rocks followed a clockwise, single-stage regional metamorphic evolution peaking at UHT conditions based on their interpretation that the age of UHT metamorphism predates the intrusion of the RIC. We suggest that the 1021 ± 23 to 999 ± 17 Ma metamorphic ages of Drüppel et al. (2013) may represent growth of zircon from crystallising melt following peak metamorphism at *ca*. 1035 Ma (Tomkins et al., 2005).

5.3. *P–T* evolution of the RVA sector

We present a revised *P–T* evolution for gneisses of the RVA Sector during the Sveconorwegian orogeny: For rocks outside the influence of the RIC (our distal sample), regional metamorphism followed a clockwise *P–T* path with peak conditions of ~850–950 °C at ~7–8 kbar followed by high-temperature, retrograde decompression to conditions of ~900 °C at 5 kbar and, subsequently, isobaric cooling to below 700 °C (Fig. 11). Whereas the distal sample preserves no compelling evidence for having experienced contact metamorphism, rocks closer to the RIC (our intermediate and proximal samples) contain evidence for a static thermal overprint (contact metamorphism) that records pressures of 3–6 kbar and reached a maximum temperature in the sample immediately adjacent to the RIC contact of over 950 °C.

The proposed *P–T* evolution outlined in this study reconciles the previous interpretations made by Degeling et al. (2001) and Drüppel et al. (2013). Degeling et al. (2001) underestimated the temperature of peak regional metamorphism by ~200 °C, due to their reliance on petrogenetic grids in the KFMASH model system, which is an oversimplification of natural rocks (White et al., 2007, 2014a), and by their use of conventional thermobarometric techniques which, due to post-peak diffusion, commonly lead to underestimates of peak temperatures (Fitzsimons and Harley, 1994; Pattison et al., 2003). Assuming our results are reliable, Drüppel et al. (2013) overestimated the temperature experienced by the rocks at Ivesdal, our intermediate locality, by ~50 °C. This is most likely due to their omission of ferric iron (modelled as O) from their model system, that affects the bulk X(Mg) of the modelled composition. In particular, these authors used an older solution model for sapphirine that does not include ferric iron, which can significantly reduce the temperature at which sapphirine is stable (Kelsey et al., 2005; Wheller and Powell, 2014). Furthermore, Drüppel et al. (2013) relied in part on spinel to constrain their *P–T* trajectories. However, the presence of elements such as Cr and Zn that are not currently incorporated into thermodynamic models, will stabilise spinel to lower temperatures than predicted by the pseudosection modelling (Tajčmanová et al., 2009).

5.4. Implications for the tectonic setting of the Sveconorwegian orogeny

The revised metamorphic evolution proposed here has implications for tectonic models for the development of the RVA Sector during the Sveconorwegian orogeny. There are at present two different tectonic models for the Sveconorwegian orogeny, a continent-continent collisional model proposed by Bingen et al. (2008) and an accretionary model of Slagstad et al. (2013a), which has been further refined by Coint et al. (2015). The collisional model postulates that at ~1140 Ma Fennoscandia collided with an as yet unidentified continent (possibly Amazonia), resulting in widespread Barrovian-type regional metamorphism. At ~930 Ma a phase of orogenic collapse was initiated that resulted in the emplacement of the RIC and formation of a regional-scale UHT contact aureole (Bingen et al., 2008). The long timescales of high-temperature conditions interpreted in this study are sufficient for the generation of high-grade metamorphic conditions within a collisional system (Clark et al., 2011). However, the lack of any obvious colliding continental block and the evidence for a series of magmatic events with arc-like chemistry that post-date the proposed collision led Slagstad et al. (2013a) to develop an alternative Andean-style accretionary model to explain the geological evolution of SW Norway. According to Slagstad et al. (2013a), the long-lived accretionary margin underwent periodic extension and compression (as a result of steep and flat slab subduction) and to alternate between periods of metamorphism (1020–990 Ma) and magmatism (1050–1020 and 990–920 Ma) to generate the SMB, HBG and RIC suites.

In contrast to the *P–T–t* proposed by Drüppel et al. (2013), which consists of a single clockwise *P–T* loop with UHT metamorphism occurring 10–15 Myr after the cessation of SMB magmatism, Slagstad and co-workers argued that the metamorphic history of rocks in SW Norway could not have been produced by a collisional orogeny (Slagstad et al., 2013b). They suggest that to generate temperatures of ~1000 °C at mid to lower crustal depths in a collisional system requires on the order of *ca*. 100 Ma (e.g. Clark et al., 2011; Clark et al., 2015).

All of the available evidence from this and previous studies indicates that a period of crustal thickening must have occurred prior to the attainment of peak regional metamorphic conditions (Bingen et al., 2008; Drüppel et al., 2013; Slagstad et al., 2013a). Possible mechanisms for crustal thickening include collision, flat-slab subduction and accretion. Whilst continental collision is a key part of the four-phase model of Bingen et al. (2008), with subduction interpreted to have ceased at 1140 Ma, this is inconsistent with the presence of the 1060–1020 Ma calc-alkaline SMB as well as the presence of contemporaneous and later arc-related features across the terranes of the Sveconorwegian Belt. These include the widespread arc geochemical signatures (Brewer et al., 2002; Andersen et al., 2007; Corfu and Laajoki, 2008; Petersson et al., 2015),

multiple periods of back-arc basin formation (Brewer et al., 2002; Söderlund and Ask, 2006; Söderlund et al., 2006; Andersen et al., 2007; Spencer et al., 2014; Petersson et al., 2015) and related bimodal magmatism (Söderlund and Ask, 2006; Bingen et al., 2008; Corfu and Laajoki, 2008; Spencer et al., 2014) as well as the overall younging to the west caused by westerly arc retreat with subduction beneath Fennoscandia (Slagstad et al., 2013a; Spencer et al., 2014 and references within; Coint et al., 2015; Petersson et al., 2015; Roberts and Slagstad, 2015).

Flat-slab subduction has been previously proposed by Slagstad et al. (2013a) to have driven crustal thickening and develop medium–*P*, high–*T* regional metamorphism within the geographically restricted area of the RVA Sector. This interpretation is consistent with magmatism starting 15 Myr prior to the onset of regional metamorphism, in which the magmas could not have been produced from partial melting related to crustal thickening (Slagstad et al., 2013a,b). Therefore, we therefore favour the Slagstad et al. (2013a) accretionary model for the RVA Sector. Similar styles of accretionary tectonics have been invoked to form regional-scale granulite facies terranes in a number of other Mesoproterozoic Orogens (Karlstrom et al., 2001; Clark et al., 2014; Korhonen et al., 2014) and have been singled out as sites of crustal growth and granulite generation throughout Earth history (Collins, 2002; Cawood and Buchan, 2007), at least since the Archaean.

More problematic is exactly how the RIC formed. Most geochronology of the RIC indicates that it was emplaced in a restricted time span at ~930 Ma. However, Coint et al. (2015) hypothesised that it may have had a protracted, episodic emplacement history based on the complex spread of zircon U–Pb ages that may record multiple intrusive events and resulted in the formation of complex growth and dissolution of zircon and monazite over an extended time interval (<1000 Ma to 920 Ma) (Möller et al., 2003 and references within). In the absence of unequivocal geochronological evidence that suggests emplacement over a prolonged period, we favour a short-lived intrusive event at ~930 Ma, with magmas emplaced into rocks that still retained small amounts of melt. Small volumes of melt in the rocks could have resulted in the reported zircon textures (Möller et al., 2003) and a single thermal pulse is consistent with the relatively simple petrographic textures documented in this study and the pluton sub-parallel isograds observed at the map scale. There is no clear evidence for slab breakoff as the causal mechanism for generation of the RIC. Recent work by Bybee et al. (2014) suggested that the RIC formed as part of a long-lived magmatic system, consistent with an accretionary setting. It is difficult to determine what caused the end of the Sveconorwegian orogeny as this margin was significantly modified during the Caledonian orogeny, leaving no obvious geological record of what previously lay to the west.

6. Conclusions

(1) Regional metamorphism in the RVA Sector during the Sveconorwegian orogeny followed a clockwise *P–T* path attaining peak conditions of ~850–950 °C and ~7–8 kbar at *ca.* 1035 Ma. Partial melting and melt loss led to the production of highly residual rock compositions.

(2) Rocks located up to at least 10 km from the RIC experienced an additional static, low-pressure, high-temperature event ~100 Myr after the peak of regional metamorphism that reached a maximum *T* of ~950 °C at 3–6 kbar. The source of this additional heat was the RIC itself, which was emplaced into slightly cooler but residual crust and resulted in the series of high-*T* isograds concentric with its margin.

(3) The collisional model of Bingen et al. (2008) cannot satisfactorily explain the metamorphic and magmatic evolution of the Sveconorwegian orogeny in the RVA Sector as it lacks a plausible heat source to drive UHT metamorphism. A model that has the Sveconorwegian Orogen as an east facing accretionary margin that experienced long-lived subduction associated with periods of flat slab subduction, rollback and arc accretion, akin to that proposed by Slagstad et al. (2013a,b) better explains the metamorphic and magmatic evolution of the RVA Sector.

Acknowledgements

We thank two anonymous reviewers for their detailed comments and Prof. M. Santosh for his editorial handling. Financial support for this project was provided by an ARC DECRA fellowship (DE120103067) to CC.

Appendix A. Supplementary data

Supplementary data related to this article can be found at http://dx.doi.org/10.1016/j.gsf.2016.07.003.

References

Andersen, T., Griffin, W.L., Pearson, N.J., 2002. Crustal evolution in the SW part of the Baltic Shield: the Hf isotope evidence. Journal of Petrology 43 (9), 1725–1747.

Andersen, T., Griffin, W.L., Sylvester, A.G., 2007. Sveconorwegian crustal underplating in southwestern Fennoscandia: LAM-ICPMS U-Pb and Lu-Hf isotope evidence from granites and gneisses in Telemark, southern Norway. Lithos 93, 273–287.

Barnichon, J.D., Havenith, H., Hoffer, B., Charlier, R., Jongmans, D., Duchesne, J.C., 1999. The deformation of the Egersund-Ogna anorthosite massif, south Norway: finite-element modelling of diapirism. Tectonophysics 303, 109–130.

Bergh, S.G., Chattopadhya, A., Ravna, E.K., Corfu, F., Kullerud, K., Swaan, K.B., Armitage, P.E.B., Myhre, P.I., Holdsworth, R.E., 2012. Was the Precambrian basement of Western Troms and Lofoten-Vesterålen in northern Norway linked to the Lewisian of Scotland? A comparison of crustal components, tectonic evolution and amalgamation history. In: Sharkov, E. (Ed.), Tectonics – Recent Advances. In Tech Open Access Publisher, pp. 283–330.

Bingen, B., Nordgulen, Ø., Viola, G., 2008. A four-phase model for the Sveconorwegian orogeny, SW Scandinavia. Norwegian Journal of Geology 88, 43–72.

Bingen, B., Skår, Ø., Marker, M., Sigmond, E.M.O., Nordgulen, Ø., Ragnhildstveit, J., Mansfeld, J., Tucker, R.D., Liégeois, J.-P., 2005. Timing of continental building in the Sveconorwegian orogen, SW Scandinavia. Norwegian Journal of Geology 85, 87–116.

Bingen, B., Stein, H.J., Bogaerts, M., Bolle, O., Mansfeld, J., 2006. Molybdenite Re–Os dating constrains gravitational collapse of the Sveconorwegian orogen, SW Scandinavia. Lithos 87, 328–346.

Bingen, B., van Breemen, O., 1998. U–Pb monazite ages in amphibolite- to granulite-facies orthogneiss reflect hydrous mineral breakdown reactions: Sveconorwegian Province of SW Norway. Contributions to Mineralogy and Petrology 132, 336–353.

Bogaerts, M., Scaillet, B., Liégeois, J.-P., Vander Auwera, J., 2003. Petrology and geochemistry of the Lyngdal granodiorite (Southern Norway) and the role of fractional crystallization in the genesis of proterozoic ferro-potassic A-type granites. Precambrian Research 124, 149–184.

Bogdanova, S.V., Bingen, B., Gorbatschev, R., Kheraskova, T.N., Kozlov, V.I., Puchkov, V.N., Volozh, Y.A., 2008. The East European craton (Baltica) before and during the assembly of Rodinia. Precambrian Research 160, 23–45.

Bol, L.C.G.M., Maijer, C., Jansen, B.H., 1989. Premetamorphic lateritisation in proterozoic metabasites of Rogaland, SW Norway. Contributions to Mineralogy and Petrology 103, 306–316.

Bolle, O., Diot, H., Liégeois, J.-P., Auwera, J.V., 2010. The Farsund intrusion (SW Norway): a marker of late-Sveconorwegian (Grenvillian) tectonism emplaced along a newly defined major shear zone. Journal of Structural Geology 32, 1500–1518.

Bolle, O., Trindade, R.I.F., Bouches, J.L., Duchesne, J.-C., 2002. Imaging downward granitic transport in the Rogaland Igneous Complex, SW Norway. Terra Nova 14, 87–92.

Brewer, T.S., Åhäll, K.I., Darbyshire, D.P.F., Menuge, J.F., 2002. Geochemistry of late mesoproterozoic volcanism in southwestern Scandinavia: implications for Sveconorwegian/Grenvillian plate tectonic models. Journal of the Geological Society, London 159, 129–144.

Brown, M., 2007. Metamorphic conditions in orogenic belts: a record of secular change. International Geology Review 49, 193–234.

Bybee, G.M., Ashwal, L.D., Shirey, S.B., Horan, M., Mock, T., Andersen, T.B., 2014. Pyroxene megacrysts in proterozoic anorthosites: implications for tectonic setting, magma source and magmatic processes at the Moho. Earth and Planetary Science Letters 389, 74–85.

Cawood, P.A., Buchan, C., 2007. Linking accretionary orogenesis with supercontinent assembly. Earth-Science Reviews 82, 217–256.
Clark, C., Fitzsimons, I.C.W., Healy, D., Harley, S.L., 2011. How does the continental crust get really hot? Elements 7, 235–240.
Clark, C., Healy, D., Johnson, T., Collins, A.S., Taylor, R., Santosh, M., Timms, N.E., 2015. Hot orogens and supercontinent amalgamation: a Gondwanan example from southern India. Gondwana Research 28 (4), 1310–1328.
Clark, C., Kirkland, C.L., Spaggiari, C.V., Oorschot, C., Wingate, M.T.D., Taylor, R.J., 2014. Proterozoic granulite formation driven by mafic magmatism: an example from the Fraser Range Metamorphics, Western Australia. Precambrian Research 240, 1–21.
Coint, N., Slagstad, T., Roberts, N.M.W., Marker, M., Røhr, T.S., Sørensen, B.E., 2015. The Late Mesoproterozoic Sirdal Magmatic Belt, SW Norway: relationships between magmatism and metamorphism and implications for Sveconorwegian orogenesis. Precambrian Research 265, 57–77.
Collins, W.J., 2002. Hot orogens, tectonic switching, and creation of continental crust. Geology 30 (6), 535–538.
Corfu, F., Laajoki, K., 2008. An uncommon episode of mafic magmatism at 1347 Ma in the mesoproterozoic Telemark supracrustals, Sveconorwegian orogen—implications for stratigraphy and tectonic evolution. Precambrian Research 160, 299–307.
Degeling, H., Eggins, S., Ellis, D.J., 2001. Zr budgets for metamorphic reactions, and the formation of zircon from garnet breakdown. Mineralogical Magazine 65 (6), 749–758.
Demaiffe, D., Michot, J., 1985. Isotope geochronology of the Proterozoic crustal segment of Southern Norway: a review. In: Tobi, A.C., Touret, J.L.R. (Eds.), The Deep Proterozoic Crust in the North Atlantic Provinces. D. Reidel Publishing Co, pp. 411–435.
Drüppel, K., Elsäßer, L., Brandt, S., Gerdes, A., 2013. Sveconorwegian mid-crustal ultrahigh-temperature metamorphism in Rogaland, Norway: U-Pb LA-ICP-MS geochronology and pseudosections of sapphrine granulites and associated paragneisses. Journal of Petrology 54 (2), 305–350.
Duchesne, J.-C., Wilmart, E., 1997. Igneous charnockites and related rocks from the Bjerkreim-Sokndal layered intrusion (Southwest Norway): a jotunite (hypersthene monzodiorite)-derived A-type granitoid suite. Journal of Petrology 38 (3), 337–369.
Duchesne, J.C., Michot, J., 1987. The Rogaland intrusive masses: introduction. In: Maijer, C., Padget, P. (Eds.), The Geology of Southernmost Norway, Norges Geologisk Undersøkelse Special Publication, vol. 1, pp. 48–59.
Falkum, T., 1982. Geologisk kart over Norge, berggrunnskart MANDAL, 1:250,000. Norges Geologisk Undersøkelse.
Falkum, T., 1985. Geotectonic evolution of southern Scandinavia in light of a late-proterozoic plate-collision. In: Tobi, A.C., Touret, J.L.R. (Eds.), The Deep Proterozoic Crust in the North Atlantic Provinces. D. Reidel Publishing Co, pp. 309–322.
Falkum, T., Petersen, J.S., 1980. The Sveconorwegian orogenic belt, a case of late-proterozoi plate-collision. Geologische Rundschau 69 (3), 622–647.
Fitzsimons, I.C.W., Harley, S.L., 1994. The influence of retrograde cation exchange on granulite P–T estimates and a convergence technique for the recovery of peak metamorphic conditions. Journal of Petrology 35 (2), 543–576.
Harlov, D.E., 2011. Petrological and experimental application of REE- and actinide-bearing accessory mineral to the study of Precambrian high-grade gneiss terrains. Geological Society of America Memoirs 207, 13–24.
Hermans, G.A.E.M., Hakstege, A.L., Jansen, J.B.H., Poorter, R.P.E., 1976. Sapphrine occurrence near Vikeså in Rogaland, Southwestern Norway. Norsk Geologisk Tidsskrift 56, 397–412.
Hermans, G.A.E.M., Tobi, A.C., Poorter, R.P.E., Maijer, C., 1975. The high-grade metamorphic Precambrian of the Sirdal-Ørsdal area, Rogaland/Vest-Agder, South-west Norway. Norges Geologisk Undersøkelse 318, 51–74.
Holland, T.J.B., Powell, R., 2011. An improved and extended internally consistent thermodynamic dataset for phases of petrological interest, involving a new equation of state for solids. Journal of Metamorphic Geology 29, 333–383.
Huijsmans, J.P.P., Kabel, A.B.E.T., Steenstra, S.E., 1981. On the structure of high-grade metamorphic Precambrian terrain in Rogaland, south Norway. Norsk Geologisk Tidsskrift 61, 183–192.
Jansen, B.H., Blok, R.J.P., Bos, M., Scheelings, M., 1985. Geothermometry and geobarometry in Rogaland and preliminary results from the Bamble area, S Norway. In: Tobi, A.C., Touret, J.L.R. (Eds.), The Deep Proterozoic Crust in the North Atlantic Provinces. D. Reidel Publishing Co, pp. 499–516.
Jansen, B.H., Tobi, A.C., 1987. Introduction to the Faurefjell metasediments. In: Maijer, C., Padget, P. (Eds.), The Geology of Southernmost Norway, Norges Geologisk Undersøkelse Special Publication, vol. 1, pp. 88–89.
Johnson, T., Brown, M., Gibson, R., Wing, B., 2004. Spinel-cordierite symplectites replacing andalusite: evidence for melt-assisted diapirism in the Bushveld Complex, South Africa. Journal of Metamorphic Geology 22, 529–545.
Johnson, T., Clark, C., Taylor, R., Santosh, M., Collins, A.S., 2015. Prograde and retrograde growth of monazite in migmatites: an example from the Nagercoil Block, southern India. Geoscience Frontiers 6 (3), 373–387.
Johnson, T.E., White, R.W., Powell, R., 2008. Partial melting of metagreywacke – a calculated mineral equilibria study. Journal of Metamorphic Geology 26, 837–853.
Karlstrom, K.E., Åhäll, K.I., Harlan, S.S., Williams, M.L., McLelland, J., Geissman, J.W., 2001. Long-lived (1.8-1.0 Ga) convergent orogen in southern Laurentia, its extensions to Australia and Baltica, and implications for refining Rodinia. Precambrian Research 111, 5–30.
Kars, H., Jansen, B.H., Tobi, A.C., Poorter, R.P.E., 1980. The metapelitic rocks of the polymetamorphic Precambrian of Rogaland, SW Norway: part II- mineral relations between cordierite, hercynite and magnetite within the osumilite-in isograd. Contributions to Mineralogy and Petrology 74, 235–244.
Kelsey, D.E., White, R.W., Powell, R., 2005. Calculated phase equilibria in K_2O–FeO–MgO–Al_2O_3–SiO_2–H_2O for silica-undersaturated sapphrine-bearing mineral assemblages. Journal of Metamorphic Geology 23, 217–239.
Korhonen, F.J., Clark, C., Brown, M., Taylor, R.J.M., 2014. Taking the temperature of Earth's hottest crust. Earth and Planetary Science Letters 408, 341–354.
Kretz, R., 1983. Symbols for rock-forming minerals. American Mineralogist 68, 277–279.
Longhi, J., Fram, M.S., Auwera, J.V., Montieth, J.N., 1993. Pressure effects, kinetics, and rheology of anorthositic and related magmas. American Mineralogist 78, 1016–1030.
Maijer, C., 1987. The metamorphic envelope of the Rogaland intrusive complex. Norges Geologisk Undersøkelse – Special Publication 1, 68–73.
Maijer, C., Andriessen, P.A.M., Hebeda, E.H., Jansen, B.H., Verschure, R.H., 1981. Osumilite, an approximately 970 Ma old high-temperature index mineral of the granulite-facies metamorphism in Rogaland, SW Norway. Geologie en Mijnbouw 60, 267–272.
Marker, M., Schiellerup, H., Meyer, G., Robins, B., Bolle, O., 2003. Introduction to the geological map of the Rogaland Anorthosite Province 1:75000. Norges Geologisk Undersøkelse – Special Publication 9, 109–116.
Möller, A., O'Brien, P.J., Kennedy, A., Kröner, A., 2002. Polyphase zircon in ultrahigh-temperature granulites (Rogaland, SW Norway): constraints for Pb diffusion in zircon. Journal of Metamorphic Geology 20, 727–740.
Möller, A., O'Brien, P.J., Kennedy, A., Kröner, A., 2003. Linking growth episodes of zircon and metamorphic textures to zircon chemistry: an example from the ultrahigh-temperature granulites of Rogaland (SW Norway). In: Vance, D., Müller, W., Villa, I.M. (Eds.), Geochronology: Linking the Isotopic Record with Petrology and Textures, The Geological Society, London, Special Publications, vol. 220, pp. 65–81.
Nijland, T.G., Maijer, C., de Haas, G.-J.L.M., 1996. The Stokkafjell Troctolite, SW Norway: its bearing on the early P-T evolution of the Rogaland terrane. Neues Jahrbuch fur Mineralogie Abhandlungen 171, 91–117.
Pasteels, P., Demaiffe, D., Michot, J., 1979. U–Pb and Rb–Sr geochronology of the eastern part of the south Rogaland igneous complex, southern Norway. Lithos 12, 199–208.
Pattison, D.R.M., Chacko, T., Farquhar, J., McFarlane, R.M., 2003. Temperature of granulite-facies metamorphism: constraints from experimental phase equilibria and thermobarometry corrected for retrograde exchange. Journal of Petrology 44 (5), 867–900.
Pearce, M.A., White, A.J.R., Gazley, M.F., 2015. TCInvestigator: automated calculation of mineral mode and composition contour for THERMOCALC pseudosections. Journal of Metamorphic Geology 33, 413–425.
Petersson, A., Scherstén, A., Bingen, B., Gerdes, A., Whitehouse, M.J., 2015. Mesoproterozoic continental growth: U–Pb–Hf–O zircon record in the Idefjorden Terrane, Sveconorwegian Orogen. Precambrian Research 261, 75–95.
Pitra, P., Waal, S.A.D., 2001. High-temperature, low-pressure metamorphism and development of prograde symplectites, marble hall fragment, Bushveld complex (South Africa). Journal of Metamorphic Geology 19 (3), 311–325.
Roberts, N.M.W., Slagstad, T., 2015. Continental growth and reworking on the edge of the Columbia and Rodinia supercontinents; 1.86-0.9 Ga accretionary orogeny in southwest Fennoscandia. International Geology Review 57, 1582–1606.
Sauer, S., Slagstad, T., Andersen, T., Kirkland, C.L., 2013. Zircon Lu-Hf Isotopes in High-alumina Orthopyroxene Megacrysts from the Neoproterozoic Rogaland Anorthosite Province, SW Norway: A Window into the Sveconorwegian Lower Crust. EGU General Assembly Conference Abstracts 15, p. 13958.
Sauter, P.C.C., 1981. Mineral relations in siliceous dolomites and related rocks in the high-grade metamorphic Precambrian of Rogaland, SW Norway. Norsk Geologisk Tidsskrift 61, 35–45.
Schärer, U., Wilmart, E., Duchesne, J.-C., 1996. The short duration and anorogenic character of anorthosite magmatism: U–Pb dating of the Rogaland complex, Norway. Earth and Planetary Science Letters 139, 335–350.
Slagstad, T., Roberts, N.M.W., Marker, M., Røhr, T.S., Schiellerup, H., 2013a. A non-collisional, accretionary Sveconorwegian orogen. Terra Nova 25, 30–37.
Slagstad, T., Roberts, N.M.W., Marker, M., Røhr, T.S., Schiellerup, H., 2013b. A non-collisional, accretionary Sveconorwegian orogen – reply. Terra Nova 25 (2), 169–171.
Söderlund, U., Ask, R., 2006. Mesoproterozoic bimodal magmatism along the Protogine Zone, S Sweden: three magmatic pulses at 1.56, 1.22 and 1.205 Ga, and regional implications. GFF 128, 303–310.
Söderlund, U., Elming, S.-Å., Ernst, R.E., Schissel, D., 2006. The Central Scandinavian Dolerite Group—protracted hotspot activity or back-arc magmatism? Constraints from U–Pb baddeleyite geochronology and Hf isotopic data. Precambrian Research 150, 136–152.
Spencer, C.J., Roberts, N.M.W., Cawood, P.A., Hawkesworth, C.J., Prave, A.R., Antonini, A.S.M., Horstwood, M.S.A., EIMF, 2014. Intermontane basins and bimodal volcanism at the onset of the Sveconorwegian Orogeny, southern Norway. Precambrian Research 252, 107–118.
Tajčmanová, L., Konopásek, J., Košler, J., 2009. Distribution of zinc and its role in the stability of spinel in high-grade felsic rocks of the Moldanubian domain (Bohemian Massif). European Journal of Mineralogy 21, 407–418.

Tobi, A.C., Hermans, G.A.E.M., Maijer, C., Jansen, B.H., 1985. Metamorphic zoning in the high-grade proterozoic of Rogaland-Vest Agder, SW Norway. In: Tobi, A.C., Touret, J.L.R. (Eds.), The Deep Proterozoic Crust in the North Atlantic Provinces. D. Reidel Publishing Co., pp. 477–497

Tomkins, H.S., Williams, I.S., Ellis, D.J., 2005. In situ U–Pb dating of zircon formed from retrograde garnet breakdown during decompression in Rogaland, SW Norway. Journal of Metamorphic Geology 23, 201–215.

Vander Auwera, J., Bolle, O., Bingen, B., Liégeois, J.-P., Bogaerts, M., Duchesne, J.-C., Waele, B.D., Longhi, J., 2011. Sveconorwegian massif-type anorthosites and related granitoids result from post-collisional melting of a continental arc root. Earth-Science Reviews 107, 375–397.

Vander Auwera, J., Bolle, O., Dupont, A., Pin, C., Paquette, J.-L., Charlier, B., Duchesne, J.-C., Mattielli, N., Bogaerts, M., 2014. Source-derived heterogeneities in the composite (charnockite-granite) ferroan Farsund intrusion (SW Norway). Precambrian Research 251, 141–163.

Vander Auwera, J., Longhi, J., 1994. Experimental study of a jotunite (hypersthene monzodiorite): constraints on the parent magma composition and crystallization conditions (P, T, f_{O2}) of the Bjerkreim-Sokndal layered intrusion (Norway). Contributions to Mineralogy and Petrology 118, 60–78.

Verschure, R.H., Andriessen, P.A.M., Boelrijk, N.A.I.M., Hebeda, E.H., Maier, W.D., Priem, H.N.A., Verdurmen, E.A.T., 1980. On the thermal stability of Rb–Sr and K–Ar biotite systems: evidence from coexisting Sveconorwegian (ca 870 Ma) and Caledonian (ca 400 Ma) biotites in SW Norway. Contributions to Mineralogy and Petrology 74, 245–252.

Versteeve, A.J., 1975. Isotope geochronology in the high-grade metamorphic Precambrian of Southwestern Norway. Norges Geologisk Undersøkelse 318, 1–50.

Westphal, M., Schumacher, J.C., Boschert, S., 2003. High-temperature metamorphism and the role of magmatic heat sources at the Rogaland anorthosite complex in Southwestern Norway. Journal of Petrology 44 (6), 1145–1162.

Wheller, C.J., Powell, R., 2014. A new thermodynamic model for sapphirine: calculated phase equilibria in K_2O-FeO-MgO-Al_2O_3-SiO_2-H_2O-TiO_2-Fe_2O_3. Journal of Metamorphic Geology 32, 287–299.

White, R.W., Powell, R., Clarke, G.L., 2002. The interpretation of reaction textures in Fe-rich metapelitic granulites of the Musgrave Block, central Australia: constraints from mineral equilibria calculations in the system K_2O-FeO-MgO-Al_2O_3-SiO_2-H_2O-TiO_2-Fe_2O_3. Journal of Metamorphic Geology 20, 41–55.

White, R.W., Powell, R., Holland, T.J.B., 2007. Progress relating to calculation of partial melting equilibria for metapelites. Journal of Metamorphic Geology 25, 511–527.

White, R.W., Powell, R., Holland, T.J.B., Johnson, T., Green, E.C.R., 2014a. New mineral activity-composition relations for thermodynamic calculations in metapelitic systems. Journal of Metamorphic Geology 32, 261–286.

White, R.W., Powell, R., Johnson, T., 2014b. The effect of Mn on mineral stability in metapelites revisited: new a–x relations for manganese-bearing minerals. Journal of Metamorphic Geology 32, 809–828.

Whitney, D.L., Evans, B.W., 2010. Abbreviations for names of rock-forming minerals. American Mineralogist 95, 185–187.

Wielens, J.B.W., Andriessen, P.A.M., Boelrijk, N.A.I.M., Hebeda, E.H., Priem, H.N.A., Verdurmen, E.A.T., Verschure, R.H., 1981. Isotope geochronology in the high-grade metamorphic Precambrian of Southwestern Norway: new data and reinterpretations. Norges Geologisk Undersøkelse 359, 1–30.

Wilmart, E., Clocchiatti, R., Duchesne, J.-C., Touret, J.L.R., 1991. Fluid inclusions in charnockites from the Bjerkreim-Sokndal massif (Rogaland, southwestern Norway): fluid origin and in situ evolution. Contributions to Mineralogy and Petrology 108, 453–462.

Wilmart, E., Duchesne, J.-C., 1987. Geothermobarometry of igneous and metamorphic rocks around the Åna-sira anorthosite massif: implications for the depth of emplacement of the South Norwegian Anorthosites. Norsk Geologisk Tidsskrift 67, 185–196.